Cable domes for self-deployable reflector antennas

Xavier Maetz, William Bettini, Jérôme Quirant, Julien Averseng, Medhi Sodki

CABLE DOMES FOR SELF-DEPLOYABLE REFLECTOR ANTENNAS

Xavier Maetz [(1) (2)], William Bettini [(1)], Jérôme Quirant [(1)], Julien Averseng [(1)], Medhi Sodki [(2)]

[(1)] Laboratoire de Mécanique et Génie Civil – UMR5508
Université de Montpellier, CC048, Place E. Bataillon, 34095 Montpellier, FRANCE
Email: xavier.maetz@umontpellier.fr
[(2)] Centre National d'Études Spatiales, 18 Avenue Edouard Belin 31401 Toulouse Cedex 4, FRANCE

***Abstract*—The LMGC team SIGECO creates and realizes innovative structures for space application in collaboration with CNES. The storage of elastic energy in flexible joints gives to these structures the advantage of being self-deployable [1]. A new concept of space reflector antennas using a deployable polygonal ring and civil engineering concepts has been recently developed [2]. A concept for CubeSats with a stowed size from 1U to 3U will be presented.**

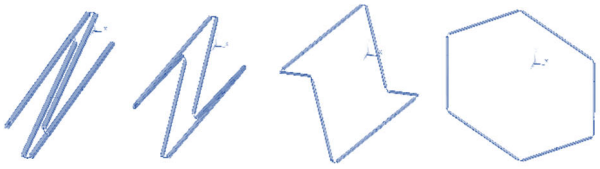

Figure 1. Deployment of the self-deployable polygonal hoop structure.

I. INTRODUCTION

Deployable reflector antennas usually consist of a rigid structure and a parabolic mesh surface for emission or reception of electromagnetic signals. This surface is often tensioned with two opposite nets linked by cables at their connection nodes. We propose a new configuration with cable domes inspired by tensegrity systems. Well-known and appreciated in civil engineering for their low mass, they could be advantageously used for space applications.

Among the existing structures, Fuller and Geiger cable domes are the most widely spread, but the tensions in elements are not homogenous in the network. A large reflector based on tensegritic diaphanous domes has been presented in 2017 by Comet Ingenieria [3]. But we propose a new kind of geometry, allowing a better distribution of tensions and a good positioning on the parabolic surface (possibly irregular). We present form-finding and static calculus for this new configuration.

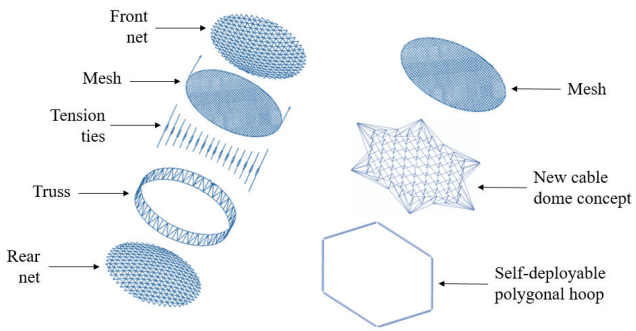

Figure 2. New configuration of space reflector antenna with cable dome compared with a classical reflector architecture like AstroMesh antenna.

The suitability of the new concept for space antennas is proposed with a complete solution. The homogenous tension in the network allows a significant optimization of the structure dimensioning. Thus, this reflector fits well with small satellites. A concept for CubeSats with a stowed size from 1U to 3U will be presented. The applications could also be relevant to auto-tensioning structures such as de-orbit or solar sails and stiff structures for solar panels support.

II. CABLE DOMES CONCEPT

Cable domes are structures inspired by tensegrity systems, which is a contraction of *tension* and *integrity*. This concept was presented for the first time in 1962 by R. B. Fuller for civil engineering applications. Cable domes only consist of bars in compressions and cables in tension, with the aim to create a dome surface. It is for this reason that these types of structures are relevant to generate paraboloid surfaces for space reflectors. Moreover, cable domes can be tensioned by an external hoop, and not a ring formed by two parallel hoops like classical tension reflectors. It allows a significant optimization of the mass and the deployment of the structure.

Fuller and Geiger cable domes are the most widely spread in civil engineering, mainly used as lightweight and large span roofs. The concept of these structures can be seen in 2D (Fig. 3). The vertical elements are

compression bars and the others are traction cables. Two opposite forces keep the cable dome stable. They represent the action of the deployed polygonal hoop on the network. The reflecting surface is attached to the top of each bar to create the desired paraboloid. It is possible to increase the number of bars to obtain a surface that fits closest to the ideal paraboloid.

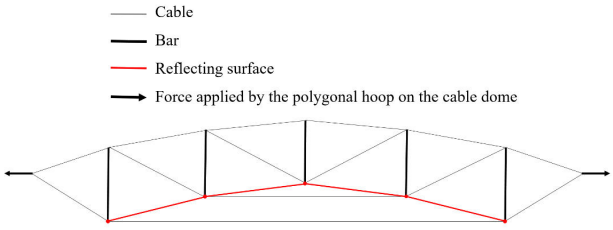

Figure 3. Geiger and Fuller cable dome 2D concept.

Geiger cable dome is a radial network. The control points which form the paraboloid are aligned with the mounts of the network (Fig. 4). Thus, the shape and the precision of the reflecting surface will depend on the number of mounts of the cable dome. It is similar to reflectors with radial deployable arms.

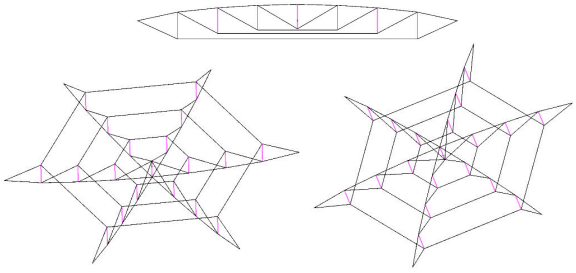

Figure 4. Geiger cable dome with 19 compression bars and 6 mounts.

Fuller cable dome is based on the same concept but the bars are arranged in diamond configuration, allowing a better distribution of the control points of the reflecting surface (Fig. 5).

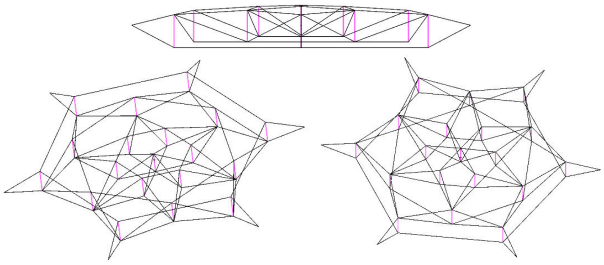

Figure 5. Fuller cable dome with 19 compression bars and 6 mounts.

It has been proved by Comet Ingenieria in [3] that deployable reflectors based on tensegrity diaphanous domes can achieve similar performances that classical tensioned reflectors in term of surface errors. A demonstrator has been built and tested in [4] and [5]. Their external structure is a ring with two parallel hoops which allows the height of the ring to be independent of the reflecting surface depth. But we propose a new kind of geometry for the network, allowing a better distribution of tensions, and supported by only one self-deployable hoop.

III. NEW PYRAMIDAL CABLE DOME CONCEPT

The new concept is directly inspired by tensegrity grids developed at the LMGC [4]. Vinicius Raducanu had proposed different typologies based on an interlacing of tensioned and compressed elements (Fig.6). The self-stressed state provides stability and rigidity to the system. Among the different solutions, the simplest and more relevant grid for a cable dome application is based on a tridirectional network in which bars are replaced by cables and vice versa.

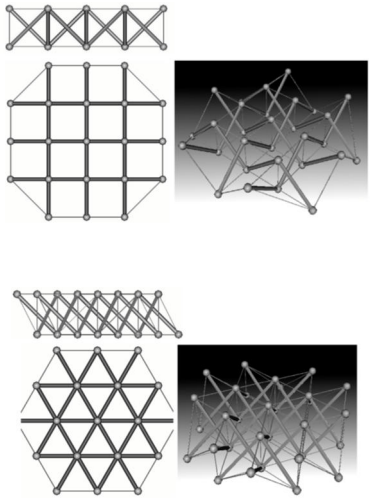

Figure 6. Tensegrity grids with bidirectional or tridirectional weaves of tilted struts.

The new cable dome is based on a statically determinate structure (isostatic). Each node in the centre of the network is kept stable with three cables in different directions (Fig. 7). The control points of the paraboloid are arranged in equilateral triangles.

The configuration of the peripheral cables depends on the number of mounts for the structure. An isostatic architecture with 6 mounts is presented in this case. More cables can be added for dynamic performance with a minor impact on the tension equilibrium.

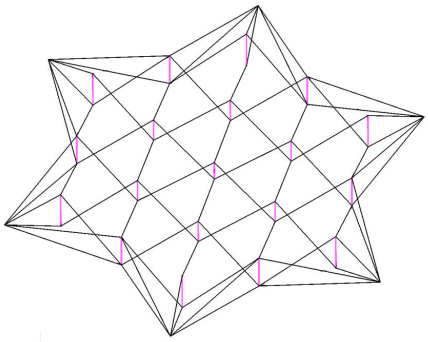

Figure 7. Pyramidal cable dome with 19 compression bars and 6 mounts.

The 2D concept of the pyramidal cable dome also differs from Geiger and Fuller structure (Fig. 8). Two opposite paraboloids are formed at the ends of the compression bars. One is convex and the other is concave. These two surfaces can be asymmetric to optimize the height of the bars. The surface opposed to the reflecting surface can even be almost flat. It is also possible to create an offset paraboloid.

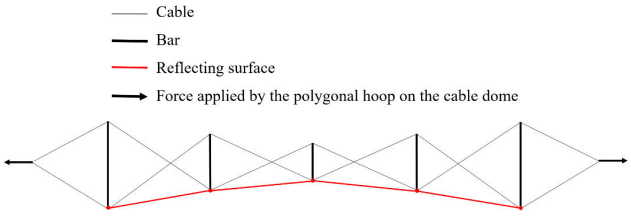

Figure 8. Pyramidal cable dome 2D concept.

Fig. 9 shows the layout of the different cable domes for a same radius R and 19 bars. Pyramidal cable dome allows a regular distribution of the control points of the paraboloid. The reflecting surface is faceted with equal equilateral triangles. Moreover, distances between consecutive bars are always uniform, which is an advantage to obtain a homogenous tension in the network.

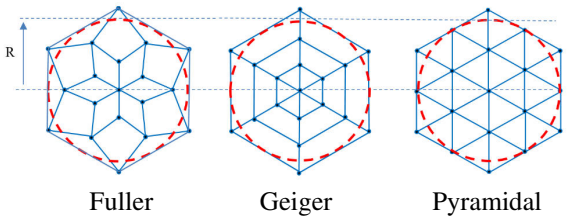

Figure 9. Layout of 19 bars for Fuller, Geiger and Pyramidal cable dome (Top view)

The number of bars of each cable dome can be calculated with the number of crowns P of the network (Tab. 1). As can be seen, the order of magnitude of the number of bars for pyramidal network is $3P^2$, by contrast with 6P for fuller and Geiger networks. Thus, pyramidal cable has more control points for a same number of crows to fit closest to the ideal paraboloid.

Fuller	Geiger	Pyramidal
6P+1	6P+1	3(P+1)P+1

Table 1. Number of bars for a same radius.

IV. STATIC ANALYSIS

In order to investigate the static performances of the pyramidal network, the study is divided into two steps. First, from the nodal equilibrium equations, the calculation formulas for the internal forces distribution can be deduced. Then, several Finite Element Models are compared with the analytical solution.

i. Geometry

The geometry presented consists of 19 bars and 6 mounts. The reflecting surface is symmetrical about its opposed surface. *T* is defined as the force applied by the polygonal hoop on the cable dome acting on each mount of the network. The internal forces of the bars, network cables, diagonal cables, and hoop cables are expressed as S_i, A_i, B_i, C_i, D_i, and E_i. The numbers 0, 1, 2, 3, and 4 are the nodes from the inner network to the outer network. 1' and 2' are the corresponding opposite nodes to 1 and 2 (Fig. 10).

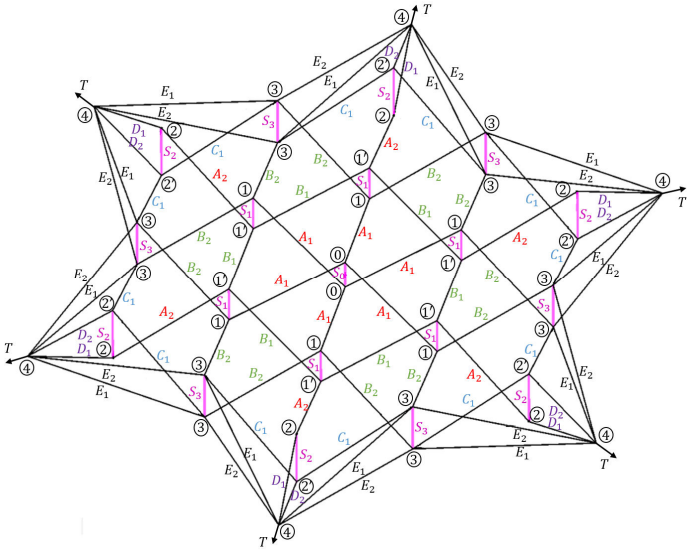

Figure 10. Geometric variables of the statically determinate pyramidal cable dome.

It is important to differentiate between cables of the inner network (A_1, A_2, B_1, B_2) where the reflecting

surface will be attached, and outer cables (C_1, E_1, E_2, D_1, D_2) which are the links with the mounts of the network. In order to have an accurate reflecting surface, inner network cables tension has to be homogenous.

The network form depends on the focal length F of the paraboloid, the height h_0 of the central bar, and the distance ΔX between two consecutive bars. Parameter d_0 is defined as the distance between a mount (node 4) and the first bar of the network. The variables αi, βi, γi, δ_i, and ϵ_i are defined as the angles from A_i, B_i, C_i, D_i and E_i to the horizontal plane. The distances Δh_1, Δh_2, and Δh_3 are the differences between the height of each bar at the nodes 1, 3, and 2, and the height of the central bar at the node 0 (Fig. 11 to 13).

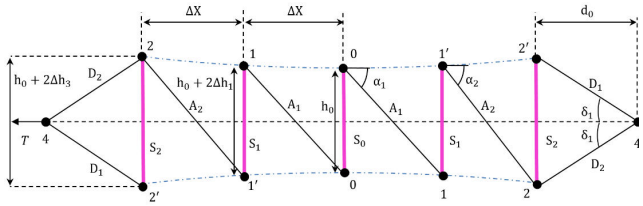

Figure 11. Profile graph in the plane containing the points 0, 1, 1', 2, 2', and 4.

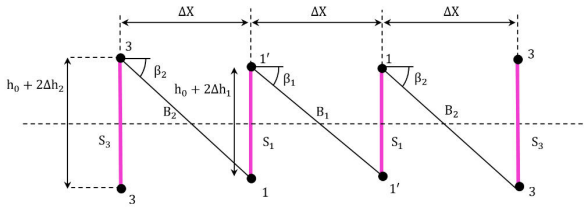

Figure 12. Profile graph in the plane containing the points 1, 1', and 3.

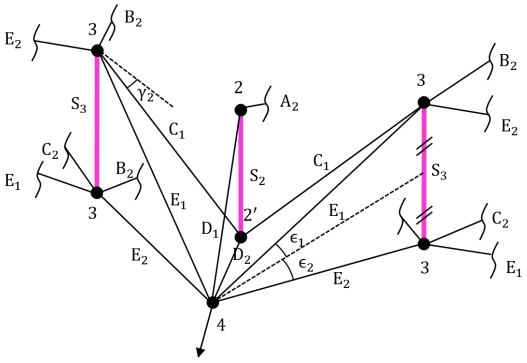

Figure 13. Graph of the statically determinate outer network.

Given the symmetry of the dome in polar coordinates, the structure can be divided into 6 equal parts along the circular direction, and for each part the distribution of components and forces are the same. In Fig. 14, χ is the angle between two cables in the inner network (in our case: $\chi = \pi / 3$), ω is the angle between two cables in the outer network, and ψ is the angle between the radial line passing through point 3 and an outer cable.

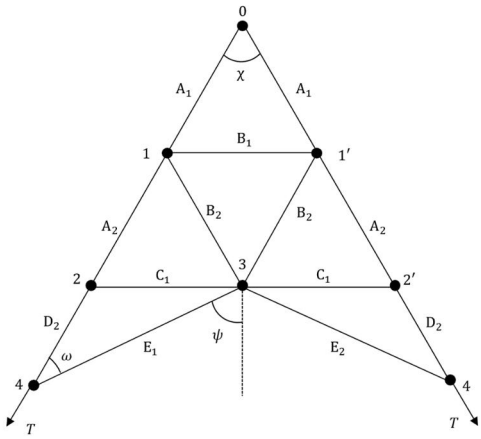

Figure 14. Graph (top view) of a part of the network.

The input parameters of the pyramidal cable dome are the height of the central bar h_0, the focal length F and the diameter of the network defined with ΔX and d_0. Then, we can calculate the length and angular parameters of the network.

Length parameters:

$$\Delta h_1 = \frac{\Delta X^2}{4F} \tag{1}$$

$$\Delta h_2 = \frac{3\Delta X^2}{4F} \tag{2}$$

$$\Delta h_3 = \frac{\Delta X^2}{F} \tag{3}$$

Angular parameters:

$$\alpha_1 = arctan\left(\frac{h_0 + \frac{\Delta X^2}{4F}}{\Delta X}\right) \tag{4}$$

$$\alpha_2 = arctan\left(\frac{h_0 + \Delta h_1 + \Delta h_3}{\Delta X}\right) \tag{5}$$

$$\beta_1 = arctan\left(\frac{h_0 + 2\Delta h_1}{\Delta X}\right) \tag{6}$$

$$\beta_2 = arctan\left(\frac{h_0 + \Delta h_1 + \Delta h_2}{\Delta X}\right) \tag{7}$$

$$\gamma_2 = arctan\left(\frac{h_0 + \Delta h_2 + \Delta h_3}{\Delta X}\right) \tag{8}$$

$$\delta_1 = arctan\left(\frac{h_0 + 2\Delta h_3}{2d_0}\right) \tag{9}$$

$$\epsilon_1 = arctan\left(\frac{h_0 + 2\Delta h_2}{2\sqrt{\left(\frac{\Delta X}{2} + d_0\right)^2 + \left(cos\left(\frac{\chi}{2}\right)\Delta X\right)^2}}\right) \tag{10}$$

$$\psi = arccos\left(\frac{d_0 \cos\frac{\pi}{6}}{\sqrt{\left(\frac{\Delta X}{2}+d_0\right)^2+\left(cos\left(\frac{\chi}{2}\right)\Delta X\right)^2}}\right) \quad (11)$$

$$\omega = \psi - \frac{\chi}{2} \quad (12)$$

ii. Equations for calculating axial forces

Equilibrium equations have been established for each node. From the internal force S_0 of the central bar, all formulas to calculate the internal force of other components can be deduced as follows:

Node 0:

$$A_1 = \underbrace{-\frac{1}{3\,sin(\alpha_1)}}_{q_0} S_0 \quad (13)$$

Node 1:

$$B_2 = \underbrace{\frac{1}{2}\frac{q_0\,cos(\alpha_1)}{cos(\beta_2)\,cos\left(\frac{\pi}{3}\right)}}_{q_1} S_0 \quad (14)$$

$$S_1 = \underbrace{-(q_0\,sin(\alpha_1)+2q_1\,sin(\beta_2))}_{q_2} S_0 \quad (15)$$

Node 1':

$$B_1 = \underbrace{-\frac{q_2}{\left(2\,sin(\beta_1)+2cos(\beta_1)\,cos\left(\frac{\pi}{3}\right)tan(\alpha_2)\right)}}_{q_3} S_0 \quad (16)$$

$$A_2 = \underbrace{\frac{2q_3\,cos(\beta_1)\,cos\left(\frac{\pi}{3}\right)}{cos(\alpha_2)}}_{q_4} S_0 \quad (17)$$

Node 2:

$$D_1 = \underbrace{\frac{q_4\,cos(\alpha_2)}{cos(\delta_1)}}_{q_5} S_0 \quad (18)$$

$$S_2 = \underbrace{-(q_4\,sin(\alpha_2)+q_5\,sin(\delta_1))}_{q_6} S_0 \quad (19)$$

Node 2':

$$D_2 = \underbrace{\frac{2\,cos(\gamma_2)\,cos\left(\frac{\pi}{3}\right)}{cos(\delta_2)}}_{q_7} C_1 \quad (20)$$

$$C_1 = \underbrace{-\frac{q_6}{2\,sin(\gamma_2)+q_7\,sin(\delta_2)}}_{q_8} S_0 \quad (21)$$

$$D_2 = \underbrace{q_7 q_8}_{q_9} S_0 \quad (22)$$

Node 3:

$$E_1 + E_2 = \underbrace{\frac{q_1\,cos(\beta_2)\,cos\left(\frac{\pi}{6}\right)}{cos(\epsilon_1)\,cos(\psi)}}_{q_{10}} S_0 \quad (23)$$

$$S_3 = \underbrace{-(q_1\,sin(\beta_2)+q_{10}\,sin(\epsilon_1)+q_8\,sin(\gamma_2))}_{q_{11}} S_0 \quad (24)$$

$$E_2 = \underbrace{\frac{q_{10}\,cos(\epsilon_1)\,sin(\psi)+q_8\,cos(\gamma_2)-q_1\,cos(\beta_2)\,sin\left(\frac{\pi}{6}\right)}{2\,cos(\epsilon_1)\,sin(\psi)}}_{q_{12}} S_0 \quad (25)$$

$$E_1 = (q_{10}-q_{12})S_0 \quad (26)$$

Node 4:

$$T = \underbrace{(2q_{10}\,cos(\epsilon_1)\,cos(\omega)+(q_5+q_9)\,cos(\delta_1))}_{q_{13}} S_0 \quad (27)$$

iii. Finite Element Models

The proposed analytical model has been benchmarked by implementing the exemplary case study in several Finite Element Models (FEM) using Patran\Nastran. The network analysed consists of 19 bars and 66 cables, having a focal length F= 4.5 m and a diameter D = 2.5 m. Different models with several heights of the central bar h_0 from 0.05 m to 0.3 m were studied.

The six mounts (node 4) of the cable dome are fully constrained. The whole network is tensioned with a force S_0 applied in the centre of the cable dome to represent the central bar. Reactions in nodes 4 are equivalent to the force T. Tab. 2 shows an example of results of the FEM and the analytical model for h_0 = 0.2 m and different forces T from 50 N to 200 N. The relative error between the two models is inferior to 0.3 %.

h_0 = 0.2 m	Force T						
	50 N		100 N		200 N		
Cables	**Ana.**	**FEM**	**Ana.**	**FEM**	**Ana.**	**FEM**	**E**
A1	10.75	10.76	21.49	21.52	42.80	42.85	0.12%
A2	11.30	11.31	22.60	22.61	45.01	45.03	0.06%
B1	10.87	10.86	21.74	21.73	43.29	43.27	0.05%
B2	11.15	11.14	22.29	22.28	44.40	44.37	0.05%
C1	6.83	6.83	13.66	13.66	27.21	27.20	0.02%
D1	10.95	10.96	21.90	21.91	43.62	43.64	0.04%
D2	6.43	6.43	12.86	12.87	25.61	25.62	0.03%
E1	10.10	10.09	20.19	20.17	40.21	40.18	0.09%
E2	11.08	11.08	22.17	22.15	44.15	44.12	0.07%
Bars	**Ana.**	**FEM**	**Ana.**	**FEM**	**Ana.**	**FEM**	**E**
S0	-10.67	-10.70	-21.34	-21.40	-42.49	-42.62	0.30%
S1	-12.81	-12.82	-25.62	-25.64	-51.03	-51.06	0.06%
S2	-9.12	-9.12	-18.24	-18.24	-36.33	-36.34	0.00%
S3	-11.62	-11.62	-23.25	-23.24	-46.30	-46.28	0.05%

Table 2. Comparison of force results between the FEM and the analytical model for h_0 = 0.2 m.

For a tension T = 100 N at each mount (node 4), the cable force range is between 12.93 N and 22.38 N. The cable tension in the inner network is homogenous. Indeed, the first crown of cables A_1 = 21.5 N and B_1 = 21.7 N (Fig. 15 yellow), and the second crown

A_2= 22.6 N and B_2 = 22.3 N (Fig. 15 orange). The bar compression range is between 18.4 N and 25.8 N.

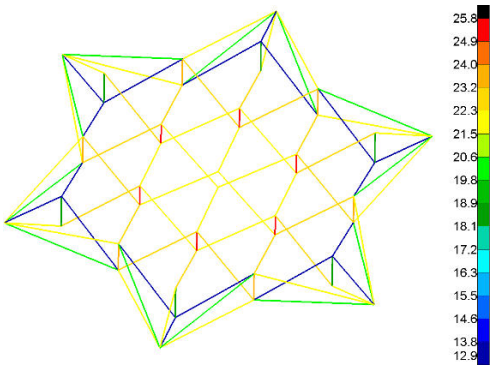

Figure 15. Force distribution in absolute value (N) h_0=0.2 m, T = 100 N.

It is possible to add some cables on the opposed side of the reflecting surface to eliminate all internal mechanism displacement modes. These cables increase significantly the dynamic performances of the network with a minor impact on the tension equilibrium. We can see on Fig. 16 the very low tension of these cables (dark blue) compared to the inner network cables (orange).

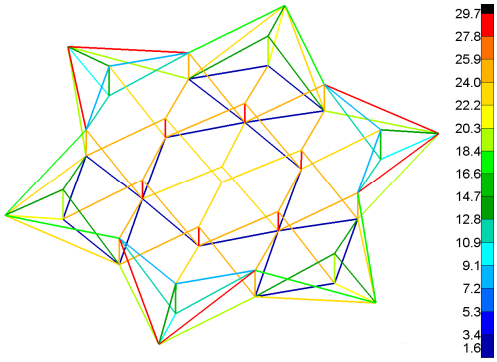

Figure 16. Force distribution in absolute value (N) h_0=0.2 m, T = 100 N.

V. APPLICATION TO CUBESATS

A self-deployable polygonal hoop coupled with a pyramidal cable dome offers a solution for CubeSat antennas. This deployable reflector mesh fits in a highly confined volume thanks to the homogenous tension in the network which allows a significant optimization of the structure dimensioning. Moreover, the network provides a good positioning of the parabolic surface by easily adding more bars in the cable dome and thus more control points. It is possible to obtain an offset fed reflecting surface or even irregular.

The concept is very scalable depending on the number of bars of the polygonal hoop and their length. The reflecting surface diameter is calculated in Tab. 2. depending on the stowed volume from 1U to 3U and the number of bars of the outer structure. The current design allows a stowage up to 24 bars in a 10 cm square (Fig.16).

		Number of bars in the polygonal hoop						
Stowage volume	Bar lenght (m)	12	14	16	18	20	22	24
1 U	0,1	0,21	0,28	0,34	0,41	0,47	0,54	0,60
1,5 U	0,15	0,40	0,50	0,59	0,69	0,79	0,88	0,98
2 U	0,2	0,59	0,72	0,85	0,97	1,10	1,23	1,36
2,5 U	0,25	0,77	0,94	1,10	1,26	1,42	1,58	1,74
3 U	0,3	0,96	1,15	1,35	1,54	1,73	1,93	2,12

Table 3. Reflecting surface diameter (m) depending on the stowed volume and the number of bars of the outer structure.

Cable dome which holds the reflecting surface will be tensioned by the deployment of the polygonal hoop. The network is not represented in fig.16 and fig.17 but fits inside the stowed outer structure. In this configuration, the network is attached to the upper joints of the polygonal hoop in order to optimize the stowage volume and to have a deployment of the cable dome in one plane. Thus, there are 12 mounts for the cable dome in a 24 bars outer structure.

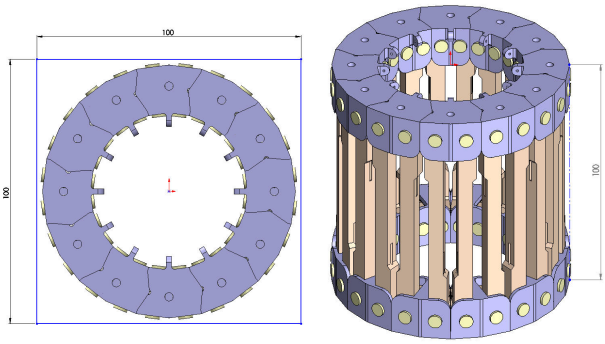

Figure 17. Stowed outer structure fitting in 1U (self-deployable polygonal hoop with 24 bars of 10 cm).

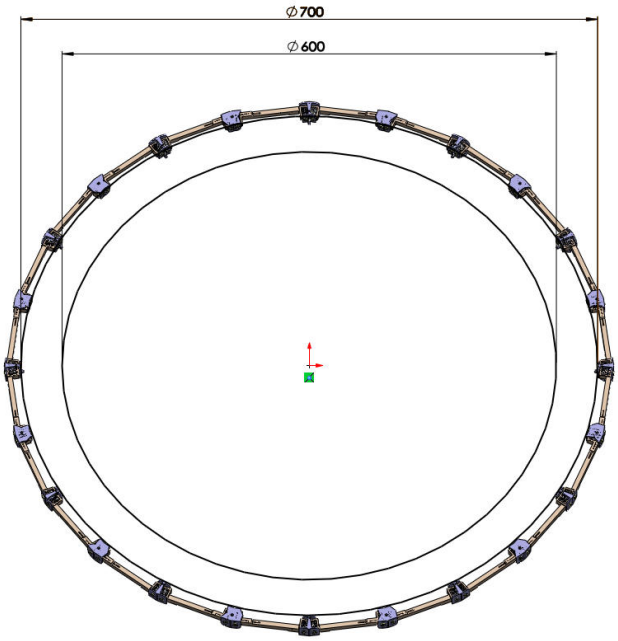

Figure 18. Deployed outer structure
(self-deployable polygonal hoop with 24 bars of 10 cm).

VI. CONCLUSION

In this paper, a novel cable dome for space reflectors has been presented in order to be integrated in a self-deployable hoop. An analytical model has been provided for the specific network geometry proposed. This new concept fits well with CubeSats to obtain a high stow-to-deployment ratio.

Future work concerns deeper analysis of RF performance achievable depending on the faceted surface accuracy and the number of bars (control points) needed. Several prototypes with different network configurations are currently being manufactured to test the deployment behaviours of the structures and the sensitivity of the surface error to the nodes position.

REFERENCES

[1] S. Morterolle, B. Maurin, J.-F. Dubé, J. Averseng, J. Quirant, “Modal behavior of a new large reflector conceptual design”, Aerospace Science and Technology, Volume 42, pp.74-79, 2015.

[2] W. Bettini, J. Quirant, J. Averseng, B. Maurin, “Self deployable geometries for space applications”, Journal of aerospace engineering, Volume 32, issue 1, 2019.

[3] J. Nieto, J. Fayos, A. Pipó, C. Montesano, E. Ozores, J. Santiago-Prowald, “Modular Deployable Structures”. Proceedings of the 38th ESA Antenna Workshop on Innovative Antenna Systems and Technologies for Future Space Missions. 3rd – 6th October 2017, Noordwijk, The Netherlands.

[4] R. Motro, V. Raducanu, “Tensegrity systems. International journal of space structures”, 18(2), p77-84, 2003

[5] J. Fayos, J. Nieto, A. Pipó and J. Santiago-Prowald. “Tensegrity diaphanous dome demonstrator”. Proceedings of the European Conference on Spacecraft Structures, Materials and Environmental Testing. 28th May – 1st June 2018, Noordwijk, The Netherlands.

[6] J. Fayos, J. Nieto, A. Pipó, G. Rodrigues, A. Ihle, J. Santiago-Prowald, “Tensegrity dome reflector demonstrator tests”. Advanced Lightweight structures and reflector antennas. 19-21 September 2018, Tbilisi, Georgia.

PDF PREPARATION AND SUBMISSION

In order to allow reasonable quality printing, please avoid excessive compression when making your PDF file. Generally, image resolutions should be 600 dpi for monochrome, 300 dpi for greyscale and colour.

VERY IMPORTANT*:* EMBED ALL FONTS and set PDF’s security method in “document properties” to “NO SECURITY”.

Deadline for submission is:

6 September 2019

Papers are to be submitted via the ESA Antenna Workshop Portal.

The file name must clearly identify the paper. Use the abstract number followed by the name of the main author (e.g. 1752728smith.pdf). Use only lower case. DO NOT name your file “XXX.pdf”.

Papers must be delivered by **6 September 2019** at the latest, to ensure inclusion in the conference proceedings.

For further information about preparing your paper, please contact:

ESA Conference Bureau
Phone: (+31) 71 565 5005
Email: esaconferencebureau@atpi.com